

## A Sandwich Porous Alumina Nanostructures Based on Anodic Alumina

Dr.Abdul Qader D. Faisal \*, Dr.Ahmed A. Moosa\* & Zeinab A. Jawad\*

Received on: 14/12/2009

Accepted on: 1/4/2010

### Abstract

A sandwich porous anodic alumina membrane (PAA/Al/PAA) films was produced using two-step anodization approach on both sides of (250)  $\mu\text{m}$  pure aluminum foil electrode as an anode. A single sheet of stainless steel or graphite was used as a cathode. Anodization on both sides of aluminum sheet was achieved. The anodization processes and pore formation were studied and discussed in this work. The produced alumina membrane (5-30)  $\mu\text{m}$  thick was analyzed using scanning electron microscopy (SEM). The SEM image shows the PAA membranes has a well-defined nanostructure. The average pore diameter reaches (25) nm. The produced  $\text{Al}_2\text{O}_3$  membrane growing on both sides of aluminum sheet was separated into a twin nano membrane.

**Keywords:** porous alumina membrane, anodization.

### التركيب النانوي لشظيرة الألومينا المسامية المبنية على أنودة الألومينا

#### الخلاصة

تم انتاج أغشية من الألومينا المسامي بطريقة الأنودة وبشكل الشظيرة (PAA/Al/PAA) باستعمال طريقة الأنودة ذات المرحلتين وعلى الجهتين لقطب من صفيحة الألمنيوم النقي بسلك 250 مايكروميتر كقطب الأنود. أستعملت صفيحة مفردة من الفولاذ او الكرافيت كقطب الكاثود. تم إجراء الأنودة على الجهتين لصفيحة الألمنيوم. دُرس في هذا البحث عمليات الأنودة وتكوين المسامات. تم تحليل أغشية الألومينا المنتجة ذات سمك حوالي (5-30) مايكروميتر باستعمال المجهر الإلكتروني الماسح (SEM). أظهرت النتائج بأن الأغشية (PAA) تمتلك تركيب نانوي. ان معدل القطر المسامي يصل الى 25 نانوميتر. ان الغشاء المنتج للألومينا على جهتي صفيحة الألمنيوم قد تم فصله الى غشائين ذا تركيب نانوي.

## Introduction

The structure of porous anodic alumina (PAA) has been known as early as 1932<sup>[1]</sup>. It consists of an array of uniformly sized straight and parallel pores. Under appropriate anodic oxidation conditions, very regular self-ordered, honeycomb-like hexagonal arrays with circular pores at the center of each hexagon can be obtained<sup>[2]</sup>.

Porous anodic aluminum oxide has become a commonly used material in many scientific fields related to nanotechnology. Their hardness, intrinsic properties, thermal and electric insulation, make them suitable for numerous applications such as sensors, filters or catalysts in biological or chemical processes or for optical device applications and in future high density recording or storage media<sup>[3]</sup>.

The laboratory-made PAA templates used for fabrication of nanomaterials are usually prepared by a self-organized two-step anodizing in an oxalic<sup>[3,4]</sup>, sulfuric<sup>[5,6]</sup> and phosphoric acid solutions<sup>[7]</sup>. However, oxalic acid as an anodizing electrolyte is frequently used. From the industrial practice point of view, the reduced costs of anodic process preparation are additional advantages of this procedure<sup>[8]</sup>.

Porous anodic alumina membranes (PAA) with a highly ordered nanopores arrangement serve as an ideal template for the formation of various nanostructure materials<sup>[4]</sup>. A typical procedure for template preparation is based on a two-step self-organized anodization of aluminum carried out at low temperature of about

(1-3) °C. PAA templates were fabricated in 0.3M oxalic acid under the anodizing potential range of (30-65) V at a relatively high electrolyte temperature ranging from 20 to 30 °C. The rate of porous oxide growth is (5-10) fold higher than in a classical mild anodization process conducted at low-temperature. Similarly at low temperature anodization, the best hexagonal pore arrangement is observed for samples anodized at 40V<sup>[9]</sup>.

A porous alumina membrane can be produced by two steps anodic oxidation process in a 0.3M oxalic acid solution for 1h at a constant applied voltage of 40V with an aluminum sheet as a counter electrode and a constant temperature of 18 °C. The first and second anodization processes were conducted under the same conditions<sup>[10]</sup>. It was found that micro-domes of porous alumina are self-assembled during anodic oxidation of an aluminum plate. These nano-pore arrays are similar to a porous alumina membrane, though the regularity of these pores is slightly worse than for the nano-pores around the micro-dome<sup>[11]</sup>. These results indicate that the porous alumina micro-domes can be used as microscale nanoporous components.

A sandwich (PAA/ Al<sub>2</sub>O<sub>3</sub>/PAA) membrane was fabricated by using the customary two-step anodization approach on both sides of an aluminum foil. A clean aluminum sheet is anodically oxidized to form an alumina membrane at 40 V and 15 °C in a solution of 0.3 mol l<sup>-1</sup> oxalic acid. Two graphite sheets are used as counter

electrodes in the two steps anodic oxidation process<sup>[12]</sup>.

The characteristics of porous alumina films produced by anodization in both oxalic acid and sulfuric acid solution were studied by Zhang<sup>[13]</sup>. The alumina films are amorphous, and the diameter of the pores for oxalic acid as electrolyte is about 60 nm and for sulfuric acid as electrolyte is about 30 nm.

A (PAA/Al/PAA) using two different anodic processes on each side of the aluminum foil was prepared by Peng et al.<sup>[14]</sup>. A novel nanostructure sandwich (PAA/Al/PAA) was successfully produced by anodic oxidation on both sides of an Aluminum foil. The pore size of the PAA membranes was controlled by choosing appropriate voltage, length of anodic oxidation time, temperature and electrolytes.

Anodic aluminum oxide (AAO) template was prepared by a two-step anodization method and cobalt particles were carefully deposited at the bottom of the pores of the template<sup>[15]</sup>. Chemical vapor deposition method was used to grow carbon nanotube (CNT's) on the template with this cobalt as catalyst and C<sub>2</sub>H<sub>2</sub> as carbon source. Well-aligned (CNT's) were obtained perpendicular to the substrate.

An inner porous anodic alumina film and an outer polyaniline/TiO<sub>2</sub> nanoparticle layer were electrochemically synthesized on an aluminum alloy by single-step, anodic polarization in an oxalic acid-based electrolyte<sup>[16]</sup>. Observation of the growth of the coating during anodic

polarization revealed that a distinct, two-layered coating is formed from the early stages of polarization, with the anodic film forming at a constant rate and the outer layer developing at a rate that decreases markedly with times beyond about 30 min.

The aim of this work is to produce a porous anodic alumina membrane using a two-step anodization process on both sides of an aluminum foil. Also to study the parameters affecting the anodizing process.

### Experimental Procedure

Aluminum sample (30 x 20 x 0.25) mm<sup>3</sup>, 99.99 % purity (Germany) was cleaned with acetone and then cleaned in ultrasonic bath with alcohol. The sample was then annealed in a quartz tube furnace (Nabertherm, Germany) at 500 °C for 3 hr in air under atmospheric pressure in order to eliminate the stresses and to obtain coarse grains for pore growth over large areas. The sample was then cleaned by degreasing with acetone and then cleaned for 5 min in an ultrasonic cleaning bath with propanol. The sample was then rinsed with distilled water and chemically etched in (5 wt. %) NaOH for 2 min.

In order to enhance the surface quality of the substrate, the aluminum foil was chemically polished in a solution of (3.5 vol. % H<sub>3</sub>PO<sub>4</sub> and 45 g/l CrO<sub>3</sub>) at 80 °C for 10 min. The aluminum sample was then anodized in an electrochemical cell as shown in Figure (1).

A stainless steel sheet (2x2x0.1) cm<sup>3</sup> was chosen as the cathode. A constant voltage of (40V) was applied

to the cell containing (0.3 mol/l oxalic acid) for 3 hrs in the temperature range (2-15) °C [controlled by ethylene glycol refrigerated bath (ULTRATEMP 2000 julabo F30), adapted with a very accurate temperature controller] to obtain a porous aluminum oxide ( $\text{Al}_2\text{O}_3$ ) on both sides of aluminum sheet. Then the anodic oxide layer ( $\text{Al}_2\text{O}_3$ ) was chemically removed in a solution of (35 ml/l 85%  $\text{H}_3\text{PO}_4$  and 20 g/l  $\text{CrO}_3$ ) at 80 °C for 10~20 min. The second anodization was conducted under the same conditions for (2, 4, 6, 8 and 10) hours respectively.

After the second anodization, the anodized aluminum sample was dipped in a phosphoric acid (5 wt.%) at 50°C for 1 min for broadening the pores. The remaining aluminum between the porous  $\text{Al}_2\text{O}_3$  sheets was removed by a solution of (0.1 M  $\text{CuCl}$  and 20 wt. %  $\text{HCl}$ ) at 5 °C for (1-8) hr in order to obtain a twin thin alumina membrane with different thicknesses.

### Results and Discussion

The current densities (J) vs. time (t) during the anodic oxidation process for the first and second anodic oxidation processes are shown in Figure (2) and (3) respectively. The two Figures give detailed information of the oxidation process for the preparation of sandwich (PAA/Al/PAA) membrane. The current density vs time curves exhibit a dramatic drops and rises of the current, followed by a current plateau corresponding to a constant anodic oxidation of the aluminum.

Figures (2) and (3) for anodic oxidation show three different stages: at

the first stage which is the initial period of anodic oxidation a compact high-resistant oxide film was formed on the aluminum substrate and the current density decreased rapidly with time.

At the second stage which starts at the minimum current density, a propagation of individual paths through the barrier layer begins and an increase in the current density is observed. As a result, a nanopores started to form. These pores will grow faster at the second step anodization. In the third stage further rearrangement of pore is indicated on the current-time curve by a local maximum. After reaching the maximum value, the current density does not change significantly with time and the porous oxide layer starts to grow on aluminum. This is indicated by the plateau where steady state pores grow and the current density becomes stable. The minimum current density for the first anodic oxidation occurs at about 20 sec while the second anodic oxidation occurs at 18 sec as shown in Figures (2) and (3) respectively. For the third stage, the first anodic oxidation occurs at 113 sec (Figure 2) and at 100 sec for the second anodic oxidation (Figure 3). A numerous pores were formed on the surface of the Al substrate. These pores are grown faster at the second step anodization process.

The data of the first stage for the first anodic oxidation and for the second anodic oxidation were fitted using a computer program. The results are shown in Figure (4a) and (4b). The data of the second stage for the first anodic oxidation and for the second anodic oxidation were fitted using a computer

program. The results are shown in Figure (5a) and (5b). The results of the computer fittings are shown in Table (1).

After fitting the first and second stage of anodic oxidation of Figure (2) and (3). The fitted data obtained are shown in Table (1).

It is clear from Table (1), the J-t curve follows an exponential relationship. This relationship is expressed as  $[J = C \exp (nt)]$  where C and n are constants and t is the time in sec. The values of C and n are the same during the first stage for the first and second anodic oxidation. The values of C and n are different during the second stage for the first and second anodic oxidation.

After the first oxidation and the removal of the initial alumina film, a texture with pits on both sides of the remained aluminum layer was formed. The stainless steel cathode was used to accelerate the dissolution of aluminum substrate. Figure (6) shows the current density vs. time for the second anodic oxidation. After 3 hrs, the current density decreases sharply and then becomes stable. During the localized pore growth and the local dissolution process, resistance of the electrode increases continuously resulting in a slow decrease in the current density. The decrease in current density with time can be expressed as:

$$J \text{ (mA/cm}^2\text{)} = 6.16 \text{ Exp } (-0.103 t)$$

Where t is the time in hrs.

When the current drops to a minimum, the formation rate of the oxide becomes equal to the local dissolution rate of the oxide barrier

layer at the bottom of the pores. The anodic oxidation reaches a new balance; accordingly, the apparent current density reaches a constant value.

Figure (7) shows an optical microscope image of the produced porous alumina layers. The optical microscope image shows the two distinct sheets of alumina. They are quite fragile materials. The thickness of the two sheets was measured optically within approximately 10µm thickness each.

The morphology of alumina membrane was observed using SEM (Carl Zeiss, Germany). Figure (8) shows the nanoporous structures of alumina membrane. The nanopore and their diameter can be recognized from these images. Figure (8a) shows very fine grains. These grains were seen by an optical microscope during the anodization processes. The pores are very small as shown in Figure (8c). The pore size was estimated to be approximately equal to (25 nm). The pore size was estimated from the SEM scales. This result was compared with the work of Lenlonek et al.<sup>[17]</sup>. The differences between the two images are due to the sample preparation technique used. They didn't use a conducting material on alumina to reveal the pores structures clear.

### Conclusions

- 1- A highly ordered nanopore arrangement of exceptional uniformity can be successfully produced using Al-sheet anodized with oxalic acid.
- 2- Two alumina membranes can be produced by controlling the

geometry of the anodizing bath such that two sides of the alumina sheet are in contact with the electrolyte. The back side needs to be masked, to avoid the masking materials.

- 3- The (J-I) relationships during the first stage for the first and second anodic oxidation processes follows an exponential decay.
- 4- The (J-I) relationship during the second stage for the first and second anodic oxidation processes follows, an exponential growth.

#### References

- [1]. Setch, S.; Miyata, A.; *Sci. Pap. Inst. Phys. Chem. Res. (Tokyo) vol 19*, 1932. PP 237.
- [2]. Masuda H.; Fukuda K.; *Science*, Vol 268, 1995. PP1466 .
- [3]. Santos A., Vojkuvka L., Pallarés J., Ferré-Borrull J. and Marsal L.F., "In Situ Electrochemical Dissolution of the Oxide Barrier Layer of Porous Anodic Alumina Fabricated by Hard Anodization", *Journal of Electroanalytical Chemistry*, 632, PP. (139-142), 2009.
- [4]. Sulka G. D. and Stepniowski W. J., "Structural Features of Self-Organized Nanopore Arrays Formed by Hard Anodization Aluminum in Oxalic Acid at Relatively High temperatures", *Journal of Electrochimica Acta*, 54, PP. (3683-3691), 2009.
- [5]. Kirchner A., Mackenzie K. J. D., Brown I. W. M., Kemmitt T. and Bowden M. E., "Structural Characterization of Heat-Treated Anodic Alumina Membranes Prepared Using A Simplified Fabrication Process", *Journal of Membrane Science*, 287, PP. (264-270), 2007.
- [6]. Zahariev A., Kanazirski I., and Girginov A., "Anodic Alumina Films Formed in Sulfuric Acid Solution", *Journal of Inorganica Chimica Acta*, 361, PP. (1789-1792), 2007.
- [7]. Inguanta R., Butera M., Sunseri C. and Piazza S., "Fabrication of Metal Nano-Structures Using Anodic Alumina Membranes Grown in Phosphoric Acid Solution", *Applied Surface Science*, 353, PP.(5447-5456), 2007.
- [8]. Ding G. Q., Shen W. Z., Zheng M. J., and Zhou Z. B., *Nanotechnology*, 17, 2590, 2006.
- [9]. Sulka G. D., "Highly Ordered Anodic Porous Alumina Formation by Self-Organized Anodizing", A. Eftekhari (Ed.), *Nanostructured Materials in Electrochemistry*, Willey-VCH, P.1, 2008.
- [10]. Tsukamoto T. and Ogino T., "Control of the Spatial Distribution of Porous Alumina Micro-Domes Formed During Anodic Oxidation", *Journal of Electrochimica Acta*, 54, PP. (4712-4717), 2009.
- [11]. Tsukamoto T., Oya T., and Ogino T., *J. Surf. Sci. Nanotechnology*, 6, 147, 2008.
- [12]. Zhao J. L. and Huang K. L., "Electrochemical Fabrication of Sandwich Nanostructures Based on Anodic Alumina", *J. Braz. Chem. Soc.*, 18, No.2, PP.(406-409), 2007.
- [13]. Zhang X. S., "Preparation of Porous Alumina by Anodization",

- Nanyang Technological Engineering, 2007.
- [14]. Peng X. S. and Chen A. C. "Electrochemical Fabrication of Novel Nanostructures Based on Anodic Alumina", Journal of Nanotechnology, 743, No.15, 2004.
- [15]. Xu J., Zhang X., Chen F., Li T., Tao X., Wang Y. and Wu X., "Preparation and Modification of Well-Aligned CNTs Grown On AAO Template", Applied Surface Science, 239, PP.(320-326), 2005.
- [16]. Zubillaga O., Cans F. J., Azkarate I., Molchan I. S., Thompson G. E. and skeldon P., "Synthesis of Anodic Films in the Presence of Aniline and TiO<sub>2</sub> Nanoparticles on AA2024-T3 Aluminium Alloy", Journal of Thin Solid Films, in press, 2009.
- [17]. Lelonek M., and Knoll M., "In situ wetting of aluminum during the growth of porous alumina by anodic oxidation", Electrochimica Acta, 53, PP. (4818-4823), 2008.

Table (1): Tabulate the fitting formulas for the 1<sup>st</sup> and 2<sup>nd</sup> anodic oxidation

Type of process	First stage (Alumina film formation), ( mA/cm <sup>2</sup> )	Second stage (Nanopores formation), ( mA/cm <sup>2</sup> )
First Anodic oxidation Figure (2)	$J = 4.96 \text{ Exp} (-0.0462t)$	$J = 1.8 \text{ Exp} (0.0097t)$
Second Anodic oxidation Figure (3)	$J = 4.96 \text{ Exp}(-0.0462t)$	$J= 1.57 \text{ Exp}(0.012t)$

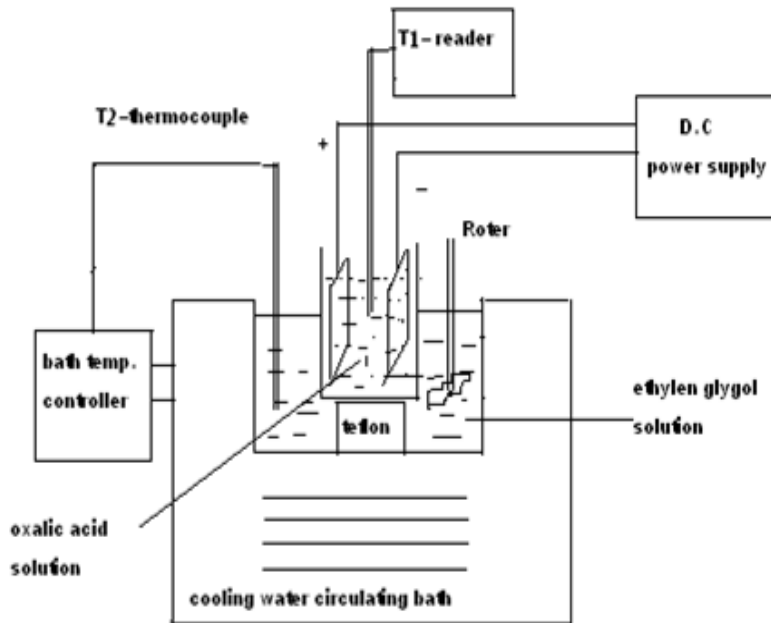


Figure (1) Schematic diagram of the electrochemical system



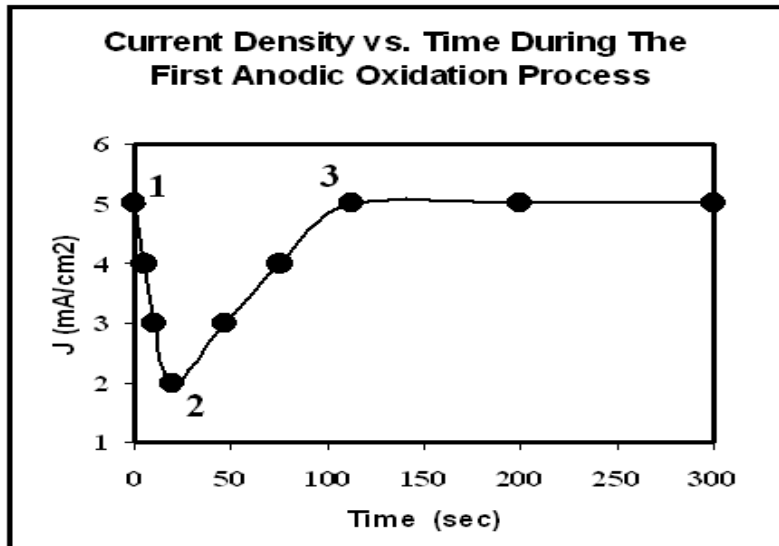


Figure (2) Current densities as a function of time during the first anodic oxidation processes at 40 V in a solution of 0.3 mol/l oxalic acid at 10 °C.

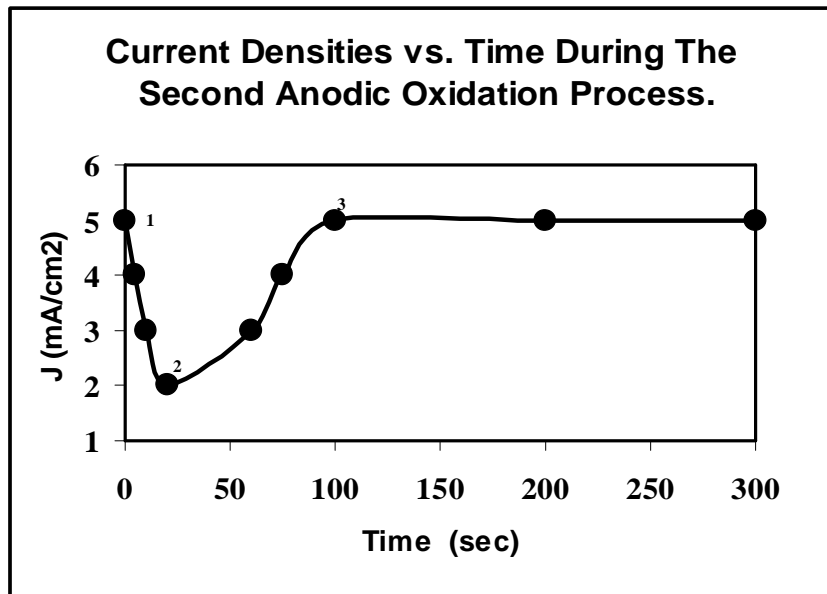


Figure (3) Current densities as a function of time during the second anodic oxidation processes at 40 V in a solution of 0.3 mol/l oxalic acid at 10 °C.

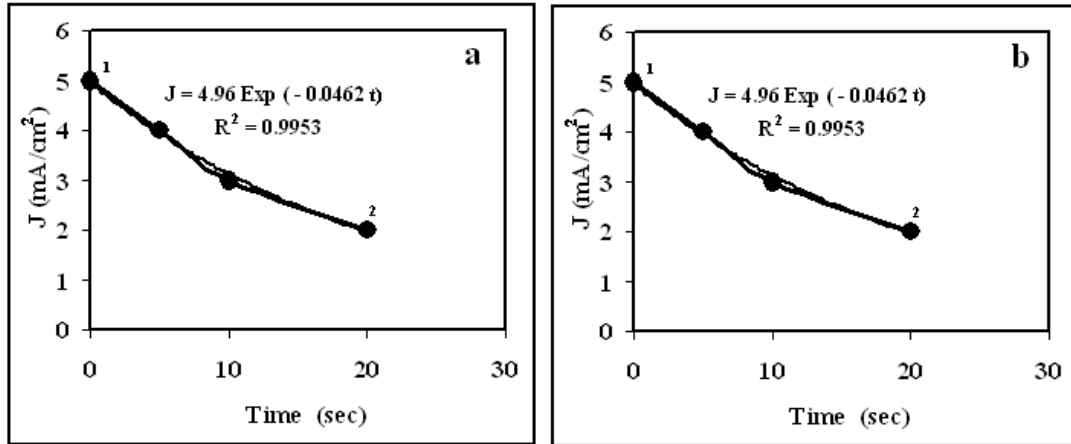


Figure (4) Current densities as a function of time during the first stage. a) For the first anodic oxidation processes, b) for the second anodic oxidation processes.

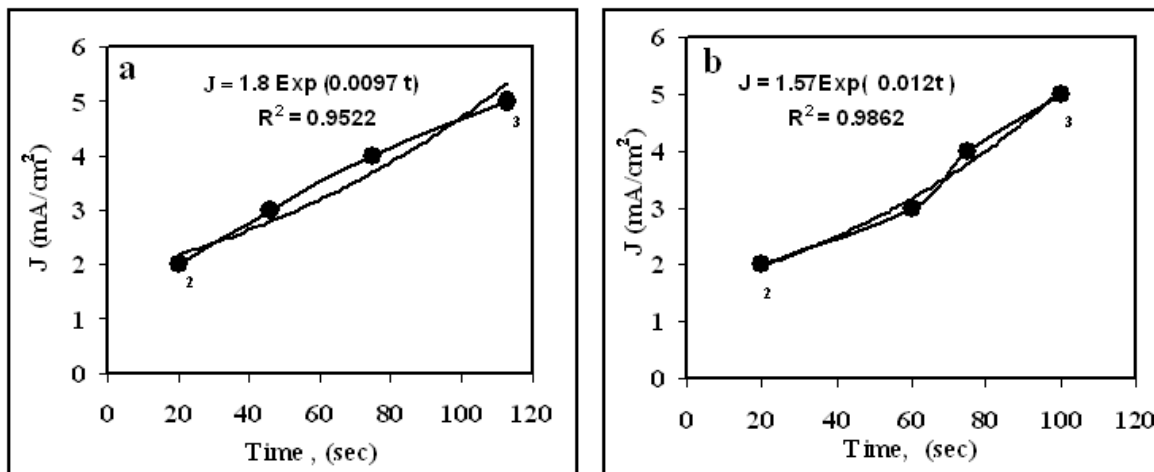


Figure (5) Current densities as a function of time during the second stage. a) For the first anodic oxidation processes, b) for the second anodic oxidation processes.

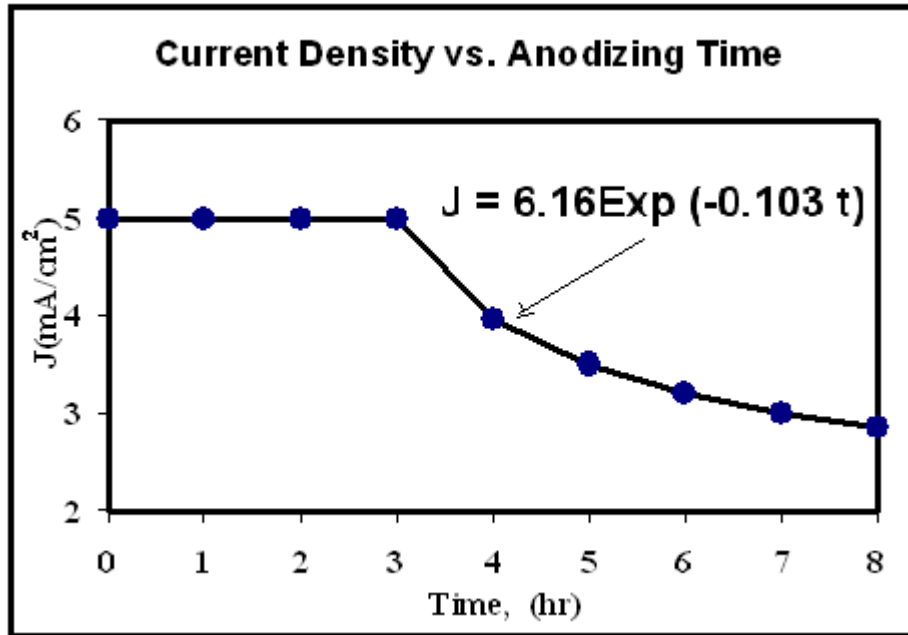
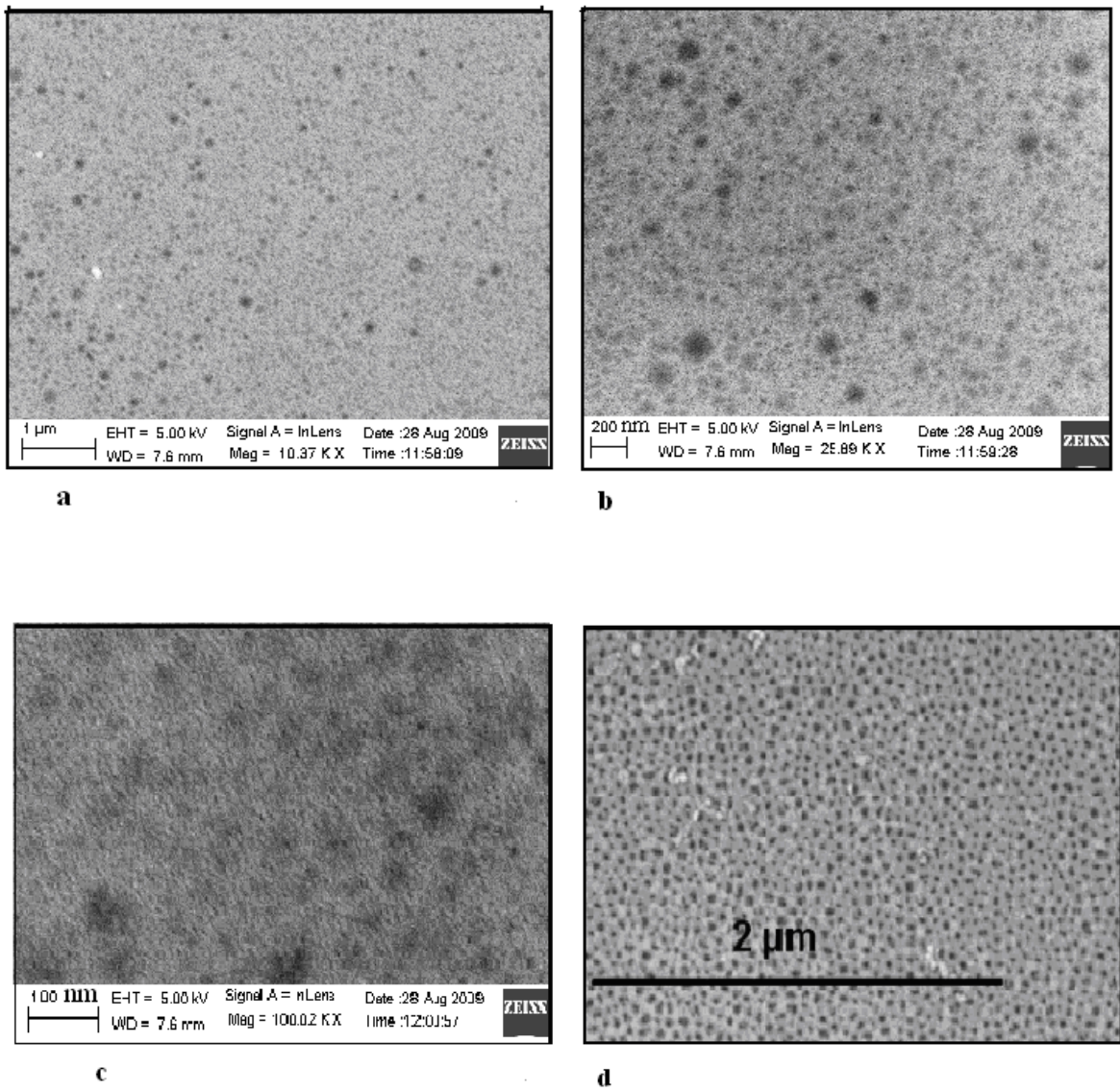


Figure (6) Current densities vs. the anodizing time during the second anodization process at 40 V in a solution of 0.3 mol/l oxalic acid at 10 °C.



Figure (7) Optical microscope image of the two distinct sheets of aluminum with measured thicknesses approximately 10µm (each).



**Figure (8)** SEM images of porous anodic alumina membrane. (a,b,c) images were taken at different magnifications . Image (d) was taken from ref. [17].